A hybrid kinematic controller for resilient obstacle avoidance of autonomous ships

IOP Conf. Series: Materials Science and Engineering **929** (2020) 012022 doi:10.1088/1757-899X/929/1/012022

A hybrid kinematic controller for resilient obstacle avoidance of autonomous ships

Mathias Marley[1,*], Roger Skjetne[1,†], Morten Breivik[2,‡] and Caroline Fleischer[3,§]

[1] Norwegian University of Science and Technology (NTNU), Department of Marine Technology, NO-7052 Trondheim, Norway
[2] Norwegian University of Science and Technology (NTNU), Department of Engineering Cybernetics, NO-7491 Trondheim, Norway
[3] Kongsberg Seatex AS, NO-7462 Trondheim, Norway

E-mail: [*]mathias.marley@ntnu.no, [†]roger.skjetne@ntnu.no, [‡]morten.breivik@ntnu.no, [§]caroline.fleischer@km.kongsberg.com.

Abstract. Resilience is an important feature of autonomous systems. To be resilient, a control system must be stable, robust, and safe. This paper explores the use of hybrid feedback controllers to ensure robustness towards uncertainties and disturbances in motion control systems for autonomous ships. Motivated by recent developments in control barrier functions (CBFs) for safe maneuvering of autonomous ships, a CBF-based hybrid kinematic controller for obstacle avoidance is proposed. The controller uses course angle as control input, making it suitable for ships with a limited speed envelope. The performance of the controller is illustrated by simulations, using an underactuated ship as a case study.

1. Introduction

Autonomous ships are inherently complex systems [1], consisting of multiple subsystems ranging from high-level mission management to low-level plant control. The control system architecture for autonomous ships may roughly be divided into three layers; mission management layer, executive guidance layer, and reactive feedback control layer, as illustrated in Figure 1. Resilience is an important objective when designing the autonomous system as a whole and the various subsystems [2], [3]. For path following of autonomous ships, the motion controller can be considered resilient if it is stable (the ship converges to and stays on the desired path), robust (with respect to uncertainties and disturbances) and safe (the ship deviates from the nominal maneuvering plan if safety demands it). In this paper we focus on safety and robustness in the reactive feedback control layer, using obstacle avoidance of an underactuated ship as a case study.

For many control problems, robustness towards noise and disturbances can only be achieved by employing some switching logic [4]. When designing control systems for autonomous ships, such problems are frequently encountered. Consider for instance the task of steering a vessel along a path while avoiding an obstacle. If the obstacle is at rest and placed exactly on the path, then passing the obstacle port or starboard is equally valid. While such a scenario cannot occur in real-life (the two options will never be exactly equal), small measurement noise in the vessel or obstacle position measurement can make the commanded action switch back and

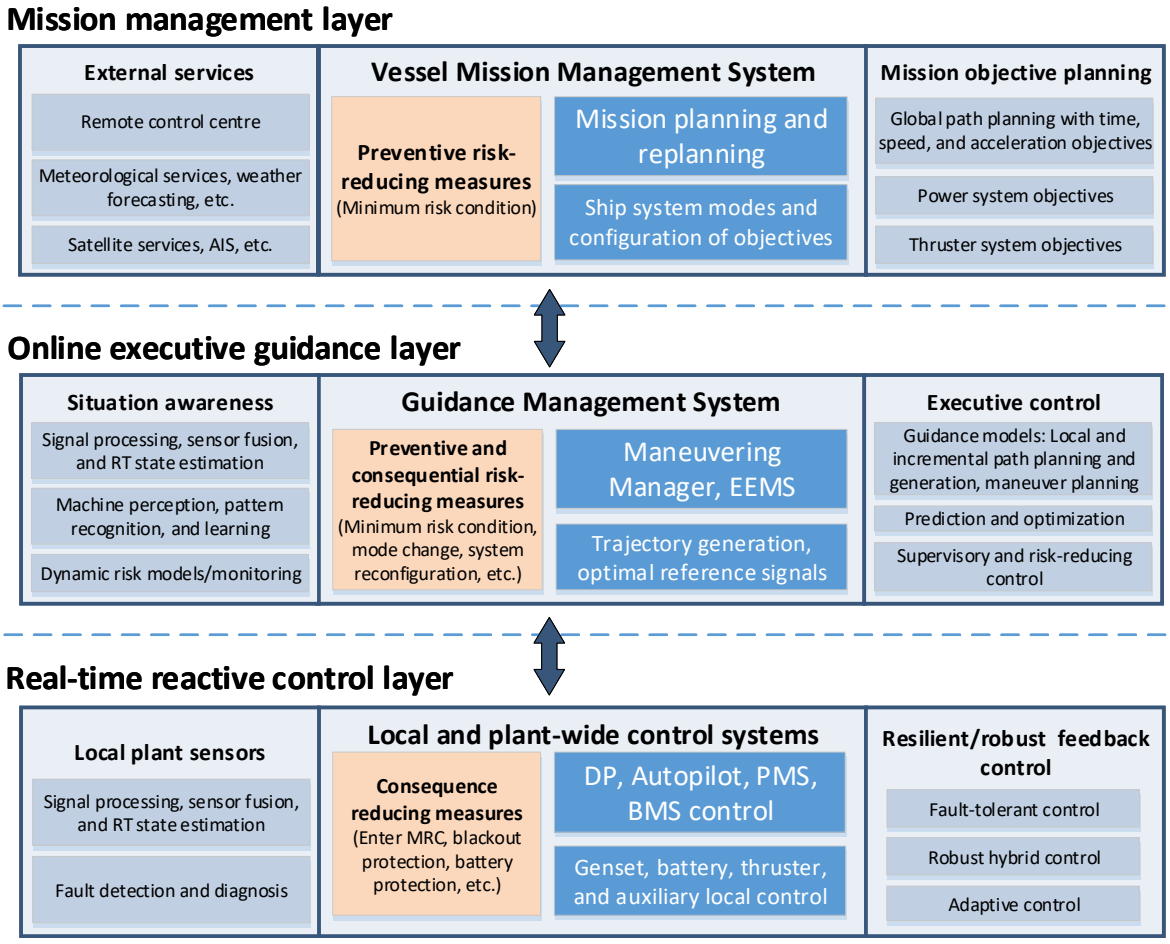

Figure 1: Example of control system architecture for autonomous ships. Abbreviations: AIS; Automatic Identification System. EEMS; Energy and Emission Management System. DP; Dynamic Positioning. PMS; Power Management System. BMS; Battery Management System. RT; Real-Time. MRC; Minimum Risk Condition. Adapted from [1].

forth indecisively between a port and starboard turn, with the result that the vessel is unable to alter the course and instead steers towards collision. In such a scenario, an experienced human captain would decide on an obstacle-free path, stick to that path and clearly show his intention, unless there is a significant change to the circumstances. Similar behavior can be built into autonomous control systems by use of intelligent switching logic. The framework of hybrid dynamical systems [5], enables systematic design of such switching logic, while providing the mathematical tools needed to formally prove stability and robustness – ensuring the overall objective of our research project; resilience in the autonomous control functions.

Significant research on obstacle avoidance has been performed as part of the Autosea project; see [6] and the references therein, where the authors propose to distinguish between global and local collision avoidance methods. Global methods construct a nominal path which is free of obstacles known prior to the mission. Local methods detect and avoid obstacles encountered during the mission, deviating from the nominal path if necessary. It is further proposed that local methods are separated into proactive and reactive methods. In reactive methods, the "evasive control inputs depend directly on the state vector through a functional relationship" [6]. While no clear definition of proactive methods is given, the context suggests that proactive

methods cannot have a continuous feedback from the state vector to the evasive control inputs. This implies that proactive methods involve having a predictive component that is used to make a plan for an evasive maneuver.

An advantage of proactive methods is the ability to come up with a consistent and smooth path for an evasive maneuver. However, problems may arise if the vessel is not able to follow the evasive path, or if the circumstances change such that the evasive path is no longer feasible and safe. The former may happen if the environmental disturbances are larger than anticipated, while the latter can occur if the encountered vessel changes its course in an unpredictable manner. In such situations, it may be necessary to abandon the initial plan for evasive maneuver.

Reactive methods may be implemented directly in the motion control system using control barrier functions (CBFs) [7]. Safety-critical controllers for autonomous vessels constructed from CBFs have recently been proposed [8], [9]. CBFs are used to design a control system that only allows control inputs that are considered safe in some sense. A CBF can be constructed such that the resulting safety-critical controller only intervenes when the evasive path planned by some higher-level proactive method is considered unsafe.

The main purpose of this paper is to explore the use of CBFs for underactuated ships with limited speed envelope. While CBF-based continuous feedback controllers can guarantee collision free operation of fully actuated vessels, the possibility of deadlock situations in perfectly symmetric conditions preclude any guarantees for task completion [10], [11]. Similarly, for vessels required to maintain a positive forward speed, safety cannot be guaranteed by continuous control. Safety can be achieved by discontinuous control. However, due to the discontinuity, arbitrarily small disturbances in the state vector can cause switching back and forth between significantly different control inputs, referred to as chattering. To ensure safety *and* robustness, a CBF-based hybrid kinematic controller is proposed. The vessel course angle is considered a virtual control input, similar to the constant avoidance angle algorithm proposed in [12]. Unlike the constant avoidance angle algorithm, a CBF-based formulation enables the use of higher derivatives of the vessel position as control input in the safety-critical controller. This is the topic of current research by the authors.

The remainder of this paper is organized as follows: In Section 2, background on hybrid control systems is provided. In section 3 a kinematic controller for obstacle avoidance is presented. Safety is ensured by using a CBF, while robustness is achieved by a hybrid feedback controller. Merging CBFs with hybrid controllers in this way is the main contribution and novelty of this paper. In Section 4, the proposed kinematic controller is used for safe maneuvering of an underactuated rudder-controlled ship. Finally, Section 5 concludes the paper.

2. Hybrid control systems

It is necessary to briefly review the concept of hybrid dynamical systems, as defined in [5]. Hybrid dynamical systems is a framework for analyzing system states that evolve both in continuous time (referred to as flow) and in discrete time (referred to as jumps). In the context of marine control systems, the physical states such as vessel position and velocity evolve by flow only, while logic variables in the control system evolve by jumps only. In [13], the hybrid systems framework is used to improve the performance of a vessel in dynamic positioning (DP) operation. The DP controller can select between several candidate controllers, depending on the state vector and an estimate of the sea state. This results in supervisory switching logic implemented as a hybrid control system.

2.1. Hybrid feedback controllers

Hybrid feedback control laws can be used for robust global stabilization of systems that cannot be globally stabilized by continuous control. Control of orientation is one such example [14]. When global stabilization by continuous control is not possible, any globally stabilizing feedback

controller must have at least one point of discontinuity. Suppose the control objective for a given system can be achieved by two different control laws, where the points of discontinuity are disjoint in the state space. Such a system may be represented by the differential equation

$$\dot{x} = f(x) + g(x)u(x, q), \tag{1}$$

where $x \in \mathbb{R}^n$ is the physical state vector and $u(x, q)$ is the hybrid feedback control law. Here, $q \in Q := \{-1, 1\}$ is a logic variable, which may take on the values $q = 1$ or $q = -1$. The switching between candidate controllers may be determined by

$$q^+ = \begin{cases} q, & P(x, q) < P_{lim}, \\ -q, & P(x, q) \geq P_{lim}, \end{cases} \tag{2}$$

where q^+ assigns the update of q after an instantaneous change (a jump). $P : \mathbb{R}^n \times Q \to \mathbb{R}$ is some indicator function which is continuous in the state vector x. q is toggled when $P(x, q)$ exceeds the threshold P_{lim}. If the indicator function consists of overlapping control Lyapunov functions (CLFs) which satisfy certain properties, rigorous robustness and stability proofs are readily available; see [15] and [16].

The challenge is often to design the indicator function such that q is toggled whenever necessary, while avoiding chattering. Since $P(x, q)$ depends on the state vector x, and not explicitly on time, the result when designed properly is a hysteresis switching mechanism.

2.2. Robust heading control

We will first illustrate the key ideas of this paper by considering heading control of a surface vessel. The yaw angular error is usually mapped to some predefined interval, typically $-\pi$ to π radians (see e.g. [17] and [18]). At the 180 degree error point, the commanded action switches between a clockwise or counterclockwise turn. At this point, arbitrarily small noise can cause chattering, which will delay convergence to the desired yaw angle[1]. To avoid a discontinuous mapping of the yaw angle to some predefined interval, the vessel heading can be represented on the unit circle, as illustrated in Figure 2. This is in many ways a more natural representation of orientation. The unit orientation vector corresponding to the yaw angle ψ, is given by

$$z^\psi := \begin{bmatrix} \cos(\psi) \\ \sin(\psi) \end{bmatrix}. \tag{3}$$

For control purposes, and neglecting the superscript, we use the orientation error vector given by

$$\tilde{z} := \begin{bmatrix} \cos(\tilde{\psi}) \\ \sin(\tilde{\psi}) \end{bmatrix}. \tag{4}$$

where $\tilde{\psi} := \psi - \psi_d$ is the yaw angular error. Controlling $\tilde{\psi} \to 0$ is equivalent to controlling $\tilde{z} \to [1\ 0]^\top$. For more details see [19].

[1] In fact, the 180 degree error point will have the characteristics of an extra (unstable) equilibrium point, implying that global stabilization of the 0 degree error point is impossible.

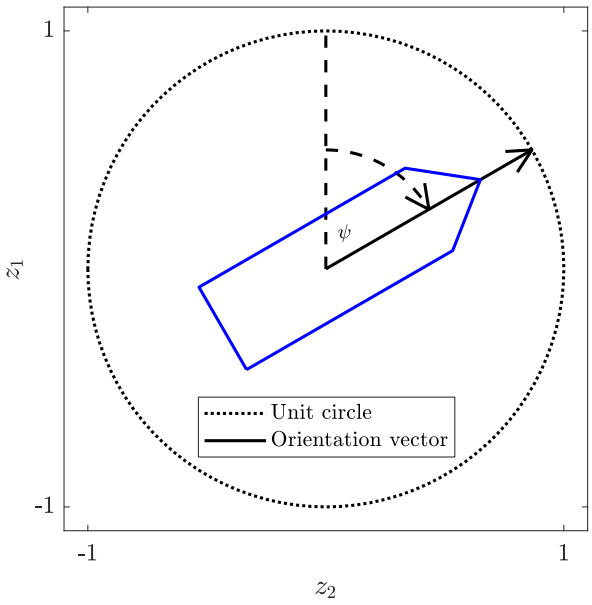

Figure 2: Vessel orientation represented on the unit circle, using the North-East-Down reference frame [20].

To introduce hysteresis, we can follow the procedure in [21] where the switching logic is constructed from two overlapping Lyapunov functions on the unit circle. The 180 degree error point is shifted in the clockwise or counterclockwise direction depending on the value of q. When $\tilde{z}$ enters some neighborhood of the 180 degree error point in the shifted coordinate system, then q is toggled. The resulting hysteresis mechanism is illustrated in Figure 3.

A similar logic may be obtained by mapping the yaw angular error to the interval $(-\pi + \alpha, \pi + \alpha]$ if $q = 1$ and $(-\pi - \alpha, \pi - \alpha]$ if $q = -1$, where $\alpha \in \mathbb{R}$ is a constant selected depending on the vessel dynamic properties and measurement quality. This mapping procedure appear simpler than using overlapping Lyapunov functions. However, since the vessel yaw rate cannot instantaneously change, a dynamic switching condition is desired, where the yaw rate and possibly higher derivatives are taken into account. Immediately the task of ensuring sufficient hysteresis width becomes more challenging. By augmenting the Lyapunov functions with additional terms based on the yaw rate and higher derivatives, a dynamic switching condition may be constructed.

When a switch occurs, there will be a discontinuity at some level in the control system. The control input should be sufficiently smooth for good performance, e.g. for a rudder controlled ship one may require that the commanded rudder angle is continuous. Sufficiently smooth actuator usage while maintaining strong formal guarantess for robustness and stability can be achieved by backstepping [15], [16]. In [22], a hybrid feedback controller for robust trajectory tracking of underactuated vehicles is proposed.

3. A kinematic controller for obstacle avoidance

We return to the example given in the introduction; steering a vessel along a path while avoiding a static obstacle. The control task is formulated as a kinematic problem. The vessel is assumed to have a constant speed, while safety is ensured by restricting the commanded orientation to a safe set, making it suitable for underactuated vessels. A CBF is used to determine the set of safe control inputs. When the nominal control input is unsafe, the CBF is said to be active and an evasive maneuver is performed. The evasive maneuver is determined by a hybrid feedback controller, giving the autonomous steering function the desired feature of resilience.

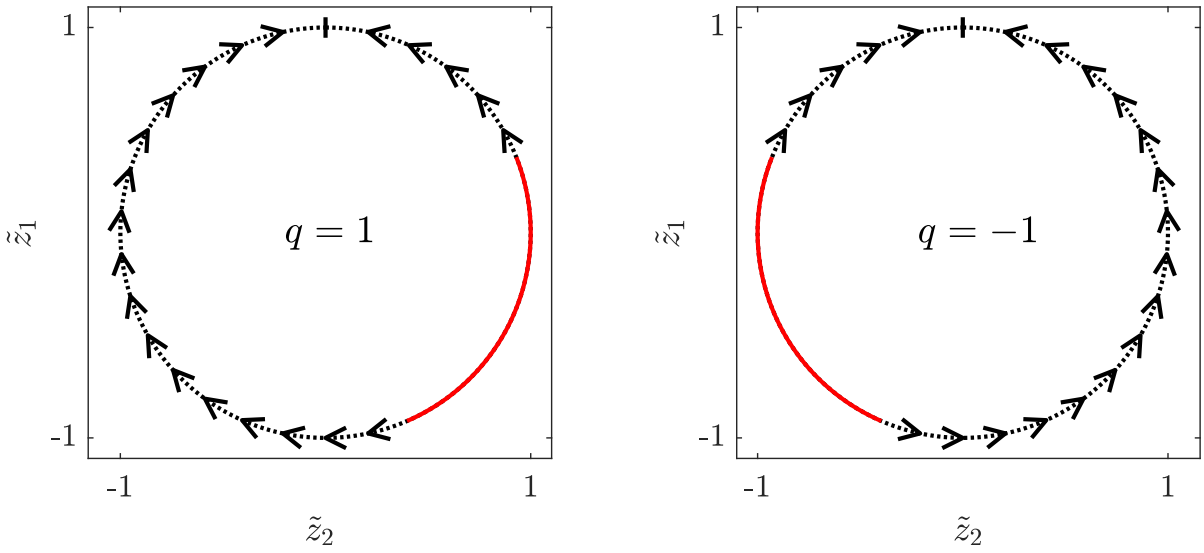

Figure 3: Illustration of the vector field for a static hysteresis mechanism for heading control which depends only on the orientation error vector $\tilde{z}$. The arrows indicate the commanded turning direction. If $\tilde{z}$ enters the sector marked by the solid red line, q is toggled and the state is governed by the other vector field. The illustration shows a hysteresis width about the 180 degree error point of 45 degrees.

3.1. Kinematic equation and problem formulation

Let $p := [x\ y]^\top$ be the vessel position in the horizontal plane, ψ the yaw angle, and $\nu := [u\ v]^\top$ the body-fixed velocity vector. The kinematic equation for motion in the horizontal plane may be written as $\dot{p} = R(\psi)\nu$, where

$$R(\psi) := \begin{bmatrix} \cos(\psi) & -\sin(\psi) \\ \sin(\psi) & \cos(\psi) \end{bmatrix} \tag{5}$$

is the rotation matrix. An alternative representation of the vessel kinematics, used in e.g. [23] and [18], is

$$\dot{p} = U z^\chi, \tag{6}$$

where $U = \sqrt{u^2 + v^2}$ is the total vessel speed and

$$z^\chi := \begin{bmatrix} \cos(\chi) \\ \sin(\chi) \end{bmatrix} \tag{7}$$

is the course orientation vector. Furthermore, $\chi := \arctan(\frac{\dot{y}}{\dot{x}}) = \psi + \beta$ is the course angle, where $\beta := \arctan(\frac{v}{u})$ is the crab angle (sometimes referred to as the sideslip or drift angle [20]).

We will consider a circular obstacle located at $p_o = [x_o\ y_o]^\top$ with radius r_o. The control task is to design a feedback controller for the desired course angle z_d^χ such that the vessel does not collide with the obstacle, deviating from the nominal path if necessary. By controlling the course angle directly, rather than the yaw angle, sideslip is automatically compensated. This is desired when performing an evasive maneuver by turning, since the crab angle during the turn will be in the direction of the obstacle (assuming low current speed and other environmental disturbances) [23].

3.2. Control system design

A CBF-based control law for obstacle avoidance in the horizontal plane is proposed, arguably in its simplest form. See [7] for an introduction to CBFs. Accordingly, we define the barrier function

$$B(p) := ||p - p_o|| - r_o, \tag{8}$$

which is negative when the vessel is in the interior of the obstacle region and positive when the vessel is outside the obstacle. Safety is ensured by enforcing

$$\dot{B} \geq -\frac{1}{T_b} B, \tag{9}$$

where

$$\dot{B} = U \frac{(p - p_o)^\top}{||p - p_o||} z^\chi \tag{10}$$

is the time derivative of B, and $T_b > 0$ is a time-constant chosen dependent on the vessel dynamic properties. The constraint (9) allows B to decrease when the vessel is far away from the obstacle, while restricting $\dot{B}$ to be non-negative when the vessel is at the boundary of the obstacle. Combining (8), (9) and (10), the set of safe orientations is obtained as

$$z^\chi_{CBF}(p, U) := \left\{ z^\chi \in \mathcal{S}^1 : U \frac{(p - p_o)^\top}{||p - p_o||} z^\chi \geq -\frac{||p - p_o|| - r_o}{T_b} \right\}, \tag{11}$$

where $\mathcal{S}^1 := \{z \in \mathbb{R}^2 : z^\top z = 1\}$ is the unit circle [21]. When the distance between the vessel and the obstacle is less than $T_b U$ meters, the set of safe orientations is restricted according to

$$z^\chi = -R(\alpha) \frac{p - p_o}{||p - p_o||}, \quad \cos\alpha \leq \frac{||p - p_o|| - r_o}{T_b U}, \tag{12}$$

where α is the relative angle between z^χ and the unit vector pointing from the obstacle towards the vessel. As the vessel approaches the obstacle, the allowable orientations become more restricted; see Figure 4 for an illustration. Define

$$\alpha_0 := \arccos\left(\frac{||p - p_o|| - r_o}{T_b U} \right), \tag{13}$$

where the range of $\arccos(\,\cdot\,)$ is defined as $[0, \pi]$, following the normal convention. The safety-critical controller is chosen as

$$z^\chi_d = \begin{cases} z^\chi_{pf}, & z^\chi_{pf} \in z^\chi_{CBF}(p, U) \\ -R(q\alpha_0) \frac{p - p_o}{||p - p_o||}, & z^\chi_{pf} \notin z^\chi_{CBF}(p, U) \end{cases}, \tag{14}$$

where z^χ_{pf} is the feedback controller for path following, while $q \in Q := \{-1, 1\}$ is a logic variable determining if the vessel shall pass the obstacle in the clockwise or counterclockwise direction. To assign the value of q, we first define the indicator function

$$P(p, z^\chi) := \frac{(p - p_o)^\top}{||p - p_o||} R\left(\frac{\pi}{2}\right) z^\chi, \tag{15}$$

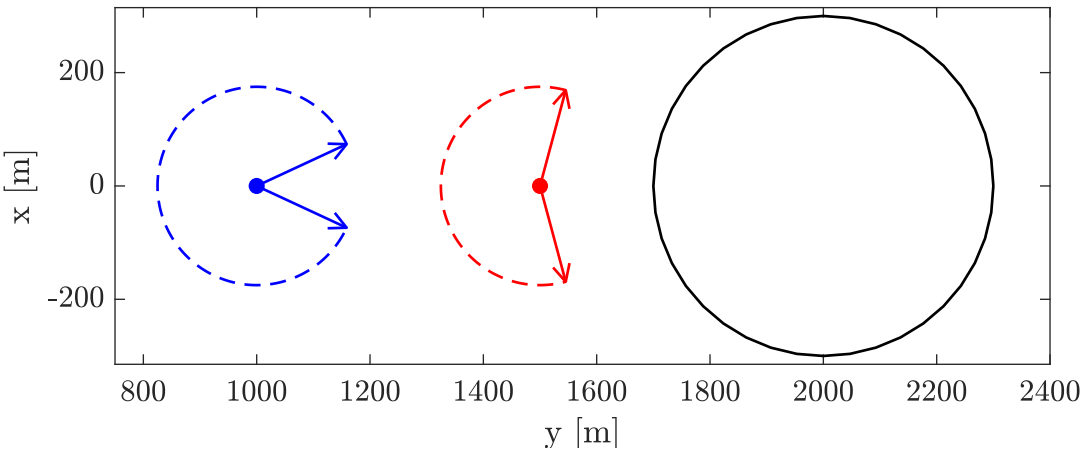

Figure 4: Illustration of the set of safe orientations constructed from the CBF. The obstacle is shown as a black circle, while the dashed circle sectors show the set z^{χ}_{CBF} for two distances (blue: 700m; red: 200m) from the boundary of the obstacle. The arrows correspond to $\pm\alpha_0$. Vessel speed $U = 7.7$m/s and time constant $T_b = 100$s.

which is negative if z^{χ} is pointing in the clockwise direction relative to the obstacle, and positive if z^{χ} is pointing in the counterclockwise direction relative to the obstacle. Choosing $q = \text{sign}(P)$ will ensure safety while minimally interfering with the path-following control objective. However, the resulting controller will be discontinuous at $P = 0$, and consequently not robust towards disturbances. Instead, we let q be given by

$$q^{+} = \begin{cases} q, & P(p, z^{\chi})q \geq -\sigma \\ -q, & P(p, z^{\chi})q < -\sigma \end{cases}, \tag{16}$$

where $0 < \sigma < 1$ is a desired hysteresis width. The combination of (14) and (16) results in a hybrid feedback controller. If σ is set to zero, this reduces to $q = \text{sign}(P)$, where sign(0) can take on both the values -1 and $+1$.

4. Case study

A case study is performed with zero and non-zero hysteresis width, to illustrate the importance of robustness. The numerical model of a Mariner class vessel provided in the Marine Systems Simulator ([24],[25]) is used in the case study. This is a 3 degree-of-freedom maneuvering model [20] of a rudder-actuated ship with length of 160m. The control input to the model is the commanded rudder angle. The model returns the vessel yaw rate and perturbation about the nominal vessel surge and sway velocity $\nu_0 = [U_0\ 0]^{\top}$, where $U_0 = 7.7$m/s is the nominal speed. No environmental disturbances are included in the numerical model.

4.1. Simulation setup

The desired path is chosen as $x = 0$, traveling in the positive y-direction. For path following, we use the line-of-sight (LOS) algorithm [20]. Following the convention in this paper, this can be formulated as

$$z^{\chi}_{pf} = z_{LOS} := \frac{1}{\sqrt{\Delta^2_{LOS} + x^2}} \begin{bmatrix} -x \\ \Delta_{LOS} \end{bmatrix}, \tag{17}$$

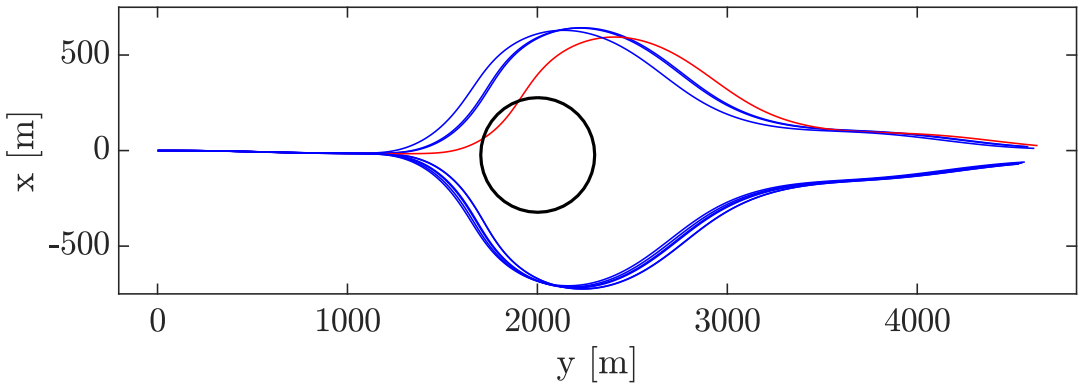

(a)

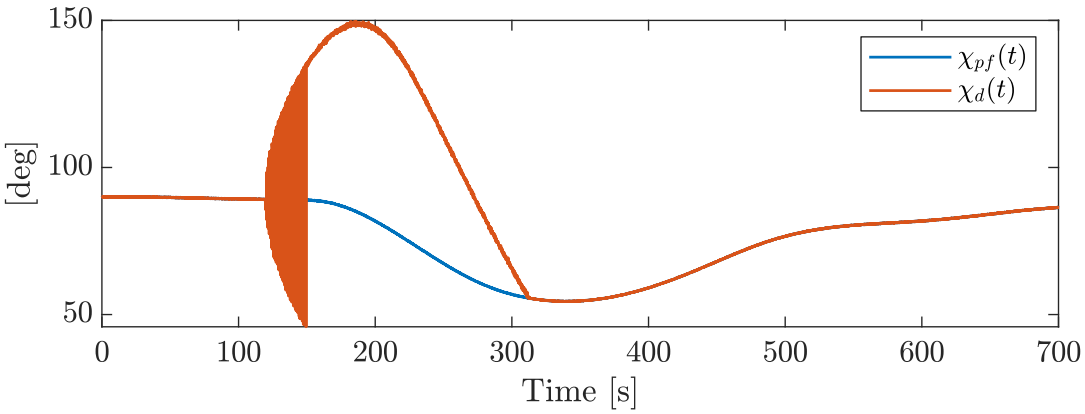

(b)

Figure 5: (a) Trajectories for 10 different runs with $\sigma = 0$. The obstacle is shown as the black circle. The ship is traveling from left to right along the positive y-axis. The trajectory which fails to avoid the obstacle is shown in red. (b) Commanded course angle for the trajectory shown in red. There is significant chattering from approximately 120 to 150s, before the ship settles on a direction to turn for the evasive maneuver. The course angle for path following is shown in blue.

with look-ahead distance set to $\Delta_{LOS} = 1000$m.

The desired course angle is given by (14), together with the switching logic (16). The evasive maneuver is initiated when $z^{\chi}_{pf} \notin z^{\chi}_{CBF}$, that is, when the desired course for path-following is considered unsafe.

An appropriate value of T_b may be determined from the maximum forward movement d_{max} of the ship during a hard turn. Choosing $T_b > d_{max}/U_0$ ensures that the set of safe orientations is restricted before the vessel is a distance d_{max} from the obstacle. d_{max} was found experimentally to be approximately 640m, giving a lower bound of $T_b = 640/7.7 \approx 83$s. In the simulations $T_b = 100$s is used, providing extra safety margin.

The control law for the rudder angle is chosen as

$$\delta_d(\tilde{\chi}, r) = -K_p(\tilde{\chi} + T_d r), \tag{18}$$

saturated by $|\delta_d| \leq 30$ degrees. Here, $\tilde{\chi} := \text{atan2}(\tilde{z}^{\chi}_2, \tilde{z}^{\chi}_1)$ is the course angular error mapped to the $[-\pi, \pi)$ interval. We note the obvious discontinuity at $\tilde{\chi} = \pm\pi$, discussed in Section 2.2.

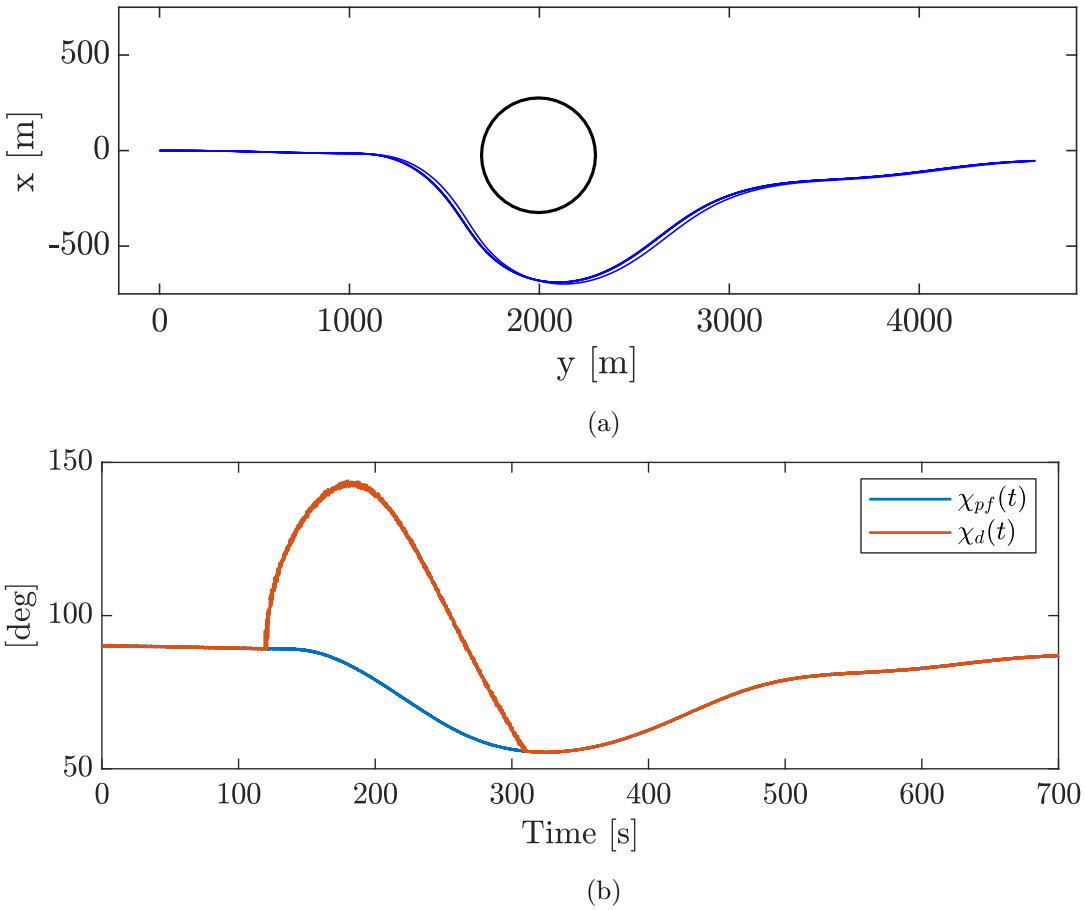

Figure 6: (a) Trajectories for 10 different runs with $\sigma = 0.05$. The obstacle is shown as the black circle. The ship is traveling from left to right along the positive y-axis. (b) Commanded course angle for one of the trajectories. The course angle for path following is shown in blue. The safety-critical controller is active from approximately 120 to 300s.

Presenting the details of a robust heading controller is outside the scope of this paper, and for the performed simulations this robustness issue did not pose any problems. The controller gains were set to $K_p = 1$ and $T_d = 10$, while $r = \dot{\psi}$ is the yaw rate[2].

Two different trials are conducted:

1) Hysteresis width $\sigma = 0$.
2) Hysteresis width $\sigma = 0.05$ and initial $q = 1$.

With $\sigma = 0$ the evasive control law has a discontinuity when z^χ is pointing directly towards the obstacle. For both trials p, U, z^χ, and p_o are corrupted by white noise. Since this results in a stochastic simulation, 10 runs are performed for each of the trials.

The obstacle is placed at $p_o = [-20\ 2000]^\top$, with radius $r_o = 300$m. The x-position of the obstacle is tuned to trigger chattering when $\sigma = 0$. For all simulations the vessel has initial position at the origin, and initial orientation along the desired path. All simulations are performed for a duration of 700s.

[2] Note that $r = \dot{\psi}$ may be replaced by $\dot{\chi}$, where $\dot{\chi}$ may be estimated from the surge and sway acceleration. Under certain assumptions on the crab angle dynamics, the control law (18) is stable using both r and $\dot{\chi}$ in the argument.

4.2. Simulation results

The trajectories from trial 1 are shown in Figure 5a. Notice the significant spread in the trajectories. For most of the runs, the ship safely passes the obstacle on either the port side or the starboard side. Out of the 10 runs, 1 fails to avoid the obstacle entirely. The commanded course angle for the run that fails to avoid the obstacle is shown in Figure 5b. Chattering is observed for a significant amount of time before the ship finally settles on a direction to turn. The chattering results in a delayed decision, leading to the vessel entering the unsafe region.

The trajectories from trial 2 are shown in Figure 6a, with corresponding commanded course angle for a selected run shown in Figure 6b. All trajectories pass the obstacle at a safe distance. Furthermore, the spread in trajectories is significantly reduced compared to trial 1 (in fact the various trajectories are barely distinguishable), which is a sign of robustness and predictability.

5. Concluding remarks

The main result of this paper is a CBF-based hybrid kinematic controller suitable for obstacle avoidance of underactuated ships. The controller addresses two of the key ingredients for resilient operation of autonomous ships; safety and robustness. The proposed controller uses a single barrier function in combination with a hybrid feedback controller. In future work, multiple overlapping barrier functions will be used, following a similar idea as the hybrid Lyapunov functions discussed in Section 2. This is a more elegant and flexible approach which enables considering higher derivatives of the vessel position as control input, such as rudder angle for rudder-controlled ships.

Acknowledgments

This work was supported by the Research Council of Norway through the Centres of Excellence funding scheme, NTNU AMOS project number 223254.

References

[1] Reddy N P, Zadeh M K, Thieme C A, Skjetne R, Sørensen A J, Aanondsen S A, Breivik M, and Eide E 2019 Zero-Emission Autonomous Ferries for Urban Water Transport: Cheaper, Cleaner Alternative to Bridges and Manned Vessels. *IEEE Electrification Magazine* **7**.4 pp. 32–45. ISSN: 23255889

[2] Baruah S, Lee P, Sarathy P, and Wolf M 2020 Achieving Resiliency and Behavior Assurance in Autonomous Navigation : An Industry Perspective. *Proceedings of the IEEE* **108**.7 pp. 1196–1207

[3] Vachtsevanos G, Lee B, Oh S, and Balchanos M 2018 Resilient Design and Operation of Cyber Physical Systems with Emphasis on Unmanned Autonomous Systems. *Journal of Intelligent & Robotic Systems* **91** pp. 59–83

[4] Sanfelice R G, Messina M J, Tuna S E, and Teel A R 2006 Robust hybrid controllers for continuous-time systems with applications to obstacle avoidance and regulation to disconnected set of points. *Proceedings of the American Control Conference*. Minneapolis, MN, USA pp. 3352–3357

[5] Goebel R, Sanfelice R G, and Teel A R 2012 *Hybrid Dynamical Systems: Modeling, Stability, and Robustness*. Princeton University Press

[6] Brekke E F, Wilthil E F, Eriksen B O H, Kufoalor D K, Helgesen K, Hagen I B, Breivik M, and Johansen T A 2019 The Autosea project: Developing closed-loop target tracking and collision avoidance systems. *J. Phys.: Conf. Ser.* **1357 01202**. ISSN: 17426596

[7] Ames A D, Coogan S, Egerstedt M, Notomista G, Sreenath K, and Tabuada P 2019 Control barrier functions: Theory and applications. *European Control Conference*. Napoli, Italy: EUCA pp. 3420–3431. arXiv: 1903.11199

[8] Basso E A, Thyri E H, Pettersen K Y, Breivik M, and Skjetne R 2020 Safety-critical control of autonomous surface vehicles in the presence of ocean currents. *IEEE Conference on Control Technology and Applications*. Montreal, Canada
[9] Thyri E H, Basso E A, Breivik M, Pettersen K Y, Skjetne R, and Lekkas A M 2020 Reactive collision avoidance for ASVs based on control barrier functions. *IEEE Conference on Control Technology and Applications*. Montreal, Canada
[10] Borrmann U, Wang L, Ames A D, and Egerstedt M 2015 Control Barrier Certificates for Safe Swarm Behavior. *IFAC-PapersOnLine* **48**.27 pp. 68–73. ISSN: 24058963
[11] Panagou D, Stipanovic D M, and Voulgaris P G 2016 Distributed Coordination Control for Multi-Robot Networks Using Lyapunov-Like Barrier Functions. *IEEE Transactions on Automatic Control* **61**.3 pp. 617–632. ISSN: 00189286
[12] Wiig M S, Pettersen K Y, and Krogstad T R 2017 A Reactive Collision Avoidance Algorithm for Vehicles with Underactuated Dynamics. *Proceedings of the IEEE Conference on Decision and Control*. Melbourne, Australia pp. 1452–1459
[13] Brodtkorb A H, Værnø S A, Teel A R, Sørensen A J, and Skjetne R 2018 Hybrid controller concept for dynamic positioning of marine vessels with experimental results. *Automatica* **93** pp. 489–497. ISSN: 00051098
[14] Bhat S P and Bernstein D S 2000 A topological obstruction to global asymptotic stabilization of rotational motion and the unwinding phenomenon. *Systems & Control Letters* **39**.1 pp. 63–70. ISSN: 07431619
[15] Mayhew C G, Sanfelice R G, and Teel A R 2011 Synergistic Lyapunov functions and backstepping hybrid feedbacks. *Proceedings of the American Control Conference*. San Francisco, CA, USA pp. 3203–3208
[16] — 2011 Further results on synergistic Lyapunov functions and hybrid feedback design through backstepping. *Proceedings of the IEEE Conference on Decision and Control and European Control Conference*. Orlando, FL, USA pp. 7428–7433
[17] Wiig M S 2019 "Collision Avoidance and Path Following for Underactuated Marine Vehicles." PhD thesis. Norwegian University of Science and Technology
[18] Hung N T, Rego F, Crasta N, and Pascoal A M 2018 Input-Constrained Path Following for Autonomous Marine Vehicles with a Global Region of Attraction. *IFAC-PapersOnLine* **51**.29 pp. 348–353. ISSN: 24058963
[19] Marley M, Skjetne R, and Teel A R 2020 Heading control of surface ships using unit circle representation. *To appear in the Proceedings of the IEEE Conference on Decision and Control*. Jeju Island, Republic of Korea
[20] Fossen T I 2011 *Handbook of marine craft hydrodynamics and motion control*. John Wiley & Sons
[21] Mayhew C G and Teel A R 2010 Hybrid control of planar rotations. *Proceedings of the American Control Conference*. Baltimore, MD, USA: IEEE pp. 154–159
[22] Casau P, Sanfelice R G, Cunha R, Cabecinhas D, and Silvestre C 2015 Robust global trajectory tracking for a class of underactuated vehicles. *Automatica* **58** pp. 90–98. ISSN: 00051098
[23] Wiig M S, Pettersen K Y, and Krogstad T R 2020 Collision Avoidance for Underactuated Marine Vehicles Using the Constant Avoidance Angle Algorithm. *IEEE Transactions on Control Systems Technology* **28**.3 pp. 951–966. ISSN: 15580865
[24] Fossen T I and Perez T 2004 *Marine Systems Simulator (Mss)*. `https://github.com/cybergalactic/MSS`. Accessed: 2020-06-05
[25] Perez T, Smogeli Ø N, Fossen T I, and Sørensen A J 2006 An overview of the marine systems simulator (MSS): A Simulink® toolbox for marine control systems. *Modeling, Identification and Control* **27**.4 pp. 259–275. ISSN: 03327353